Research Article

Received: 30 August 2013 Revised: 16 December 2013 Accepted article published: 4 February 2014 Published online in Wiley Online Library: 19 March 2014

(wileyonlinelibrary.com) DOI 10.1002/ps.3755

Glyphosate-resistant and glyphosate-susceptible Palmer amaranth (*Amaranthus palmeri* S. Wats.): hyperspectral reflectance properties of plants and potential for classification

Krishna N Reddy,[a*] Yanbo Huang,[a] Matthew A Lee,[a] Vijay K Nandula,[a] Reginald S Fletcher,[a] Steven J Thomson[a] and Feng Zhao[b]

Abstract

BACKGROUND: Palmer amaranth (*Amaranthus palmeri* S. Wats.) is a troublesome agronomic weed in the southern United States, and several populations have evolved resistance to glyphosate. This paper reports on spectral signatures of glyphosate-resistant (GR) and glyphosate-sensitive (GS) plants, and explores the potential of using hyperspectral sensors to distinguish GR from GS plants.

RESULTS: GS plants have higher light reflectance in the visible region and lower light reflectance in the infrared region of the spectrum compared with GR plants. The normalized reflectance spectrum of the GR and GS plants had best separability in the 400–500 nm, 650–690 nm, 730–740 nm and 800–900 nm spectral regions. Fourteen wavebands from within or near these four spectral regions provided a classification of unknown set of GR and GS plants, with a validation accuracy of 94% for greenhouse-grown plants and 96% for field-grown plants.

CONCLUSIONS: GR and GS Palmer amaranth plants have unique hyperspectral reflectance properties, and there are four distinct regions of the spectrum that can separate the GR from GS plants. These results demonstrate that hyperspectral imaging has potential application to distinguish GR from GS Palmer amaranth plants (without a glyphosate treatment), with future implications for glyphosate resistance management.
Published 2014. This article is a U.S. Government work and is in the public domain in the USA.

Keywords: glyphosate-resistant weeds; herbicide-resistant weeds; hyperspectral imaging; Palmer amaranth; weed classification

1 INTRODUCTION

Glyphosate [*N*-(phosphonomethyl) glycine] is the most widely used herbicide in the world, in large part because of its application in transgenic, glyphosate-resistant cropping systems.[1] Glyphosate use (both in frequency and amount) has increased in glyphosate-resistant (GR) corn, cotton and soybean. Repeated and intensive use of glyphosate has exerted a high selection pressure on weed populations, resulting in evolution of GR weeds. To date, a total of 25 weed species, including Palmer amaranth (*Amaranthus palmeri* S. Wats.), have evolved resistance to glyphosate worldwide.[2] GR Palmer amaranth was first reported in Georgia in 2006.[3] Since then, 18 other states in the United States have reported GR Palmer amaranth populations.[2]

GR Palmer amaranth is a troublesome weed in corn, cotton and soybean. It can emerge throughout the growing season, grow rapidly, reaching heights in excess of 2 m, quickly overtopping crops such as cotton and soybean, and reduce yield and harvest efficiency.[3,4] Not all Palmer amaranth field populations are resistant to glyphosate. GR and glyphosate-sensitive (GS) Palmer amaranth plants look alike, and visually it is impossible to distinguish GR plants from GS plants.

Currently, GR and GS plants are identified by assessing physiological and biochemical changes in plants following glyphosate treatment. Whole plants, single leaves or leaf discs are subjected to glyphosate treatment to identify GR from GS plants. Glyphosate-treated GS plants develop visible injury symptoms (chlorosis, necrosis) and are killed, while GR plants survive glyphosate treatment, with the duration to survival dependent on glyphosate resistance mechanism(s) and prevailing growing

* *Correspondence to: Krishna N Reddy, USDA-ARS, Crop Production Systems Research Unit, 141 Experiment Station Road, Stoneville, Mississippi 38776, USA. E-mail: Krishna.Reddy@ars.usda.gov*

a *USDA – Agricultural Research Service, Crop Production Systems Research Unit, Stoneville, MS, USA*

b *School of Instrumentation Science and Opto-electronics Engineering, Beihang University, Beijing, China*

Published 2014. This article is a U.S. Government work and is in the public domain in the USA.

conditions. In a leaf-dip assay, where a single leaf is dipped in glyphosate solution for 48 h and leaf injury (wilting and discoloration) is visually estimated,[5] leaves of GS plants exhibit greater injury than leaves of GR plants. An *in vivo* shikimate accumulation assay with leaf discs following glyphosate treatment is often used to distinguish GR from GS plants.[6] In most cases, GS plants accumulate higher levels of shikimate, and lower levels of shikimate or a lack thereof in GR plants indicate resistance to glyphosate.

Whole-plant and leaf-dip or leaf-disc shikimate assays, while undoubtedly reliable in distinguishing GR from GS plants, are tedious and labor intensive. Hyperspectral technology involves using sensors that collect spectral data across a wide range of the optical spectrum at a high spectral resolution, allowing for detailed spectral signatures of an object. This technology has been used in many agricultural studies, including identification of plant stress caused by drought, nutrient deficiencies, pest infestations and herbicide applications.[7] There have been studies on weeds in which the locations of agricultural weeds were mapped using hyperspectral technology,[8,9] but the authors are not aware of any studies where this technology has been used to address its utility in differentiating GR and GS weeds. The mechanisms involved in glyphosate resistance in GR Palmer amaranth may affect its leaf chemical composition. Differences in chemical composition in turn could affect light absorption patterns in GR and GS plants. It was hypothesized that there could be differences in hyperspectral reflectance properties between GR and GS plants. The specific objectives of the present study were (1) to characterize the hyperspectral reflectance properties of GR and GS Palmer amaranth plants and (2) to assess classification accuracy of an unknown set of plants (test set) using the analysis of data from a known set of plants (training set).

2 MATERIALS AND METHODS

2.1 Greenhouse study

2.1.1 Genetically heterogeneous GR and GS Palmer amaranth plants

GR and GS Palmer amaranth biotypes from Mississippi[10] were raised from seed and used in the study during September–October 2012. Seeds were planted at 1 cm depth in 50 × 20 × 6 cm plastic trays with holes that contained a commercial potting mix (Metro-Mix 360; Sun Gro Horticulture, Bellevue, WA). Two weeks after emergence, Palmer amaranth plants were transplanted into 10 × 10 × 10 cm pots containing the potting mix mentioned before. Plants were fertilized once with a nutrient solution (Miracle-Gro; The Scotts Company LLC, Marysville, OH) containing 200 mg L^{-1} each of N, P_2O_5 and K_2O 1 week after transplanting, and were subirrigated as needed. The greenhouse was maintained at 28/22 ± 3 °C day/night temperature, with natural light supplemented by sodium vapor lamps to provide a 12 h photoperiod. GR and GS plants, both at the 6–7-leaf growth stage (10–15 cm tall), were used for reflectance measurements.

2.1.2 Genetically homogeneous GR and GS Palmer amaranth plants

Plants propagated via cloning (Hoagland RE, private communication, 2013) were used in the study during November–December 2012. Seeds were collected from the area around Stoneville, Mississippi (two GR populations), and two areas in Georgia (two GS populations). The plants were cloned from individual parents by excising petioles of branch points and immediately placing the excised tissue sections in deionized water. The excised tissue was then removed from the deionized water and dried with a towel. The cut tips were then coated with rooting hormone powder (1.6%; Hormex, Brooker Chemicals, Hollywood, CA) and planted in moistened vermiculite/peat (Sun Gro Horticulture, Bellevue, WA) potting mixture. After about 7 days to allow root initiation and growth, the clones were transplanted into large pots (15 cm in diameter by 15 cm in height) containing soil and placed in a greenhouse under similar growing conditions as described before. The plants were in the early flowering stage when they were imaged.

2.2 Field study

Previously characterized[10] GR and GS plants were grown in the greenhouse as described for genetically heterogeneous plants. Eighty plants each of GR and GS, 10–15 cm tall, were transplanted in the field at the USDA-ARS Crop Production Systems Research Unit farm, Stoneville, Mississippi, on 10 July 2013. Plants were watered as needed and allowed to establish. Hyperspectral reflectance measurements were taken on 1–2 August 2013, and plants were about 75–120 cm tall.

2.3 Plant hyperspectral imaging

2.3.1 Greenhouse study

Two sets of plants were imaged using hyperspectral sensors. The first set of plants (27 GS and 25 GR) were from heterogeneous populations. The second set of plants (61 GS and 72 GR) were from genetically homogeneous populations. A Resonon Pika II hyperspectral camera (Resonon, Bozeman, MT) mounted on a stand was used to capture images of the Palmer amaranth plants. The Pika II camera is a push-broom hyperspectral sensor with a spectral range of 394.300–896.917 nm in 240 wavelength bands. An objective lens with a 23 mm focal length gave the camera a 12° field of view. As the camera was held about 66 cm above the plants, the spatial resolution of the images was about 0.24 × 0.24 mm $pixel^{-1}$. This set-up permitted imaging of one plant every minute. The high spatial resolution permitted a large number of pure plant pixels to be collected and analyzed. Taller plants were closer to the artificial light source (provided by four 35 W 12 VDC incandescent light bulbs) and thus were exposed to greater light intensity than the white reference, which was collected at floor level. To ameliorate this effect whenever possible, plants of approximately the same age were imaged, so that the distance between the plants and the camera was nearly always the same. Effects of height differences were normalized in the image processing step.

2.3.2 Field study

The camera described in the greenhouse study was used to image the plants in the field. The camera was mounted on a three-point hitch on a tractor, flexible to move vertically and horizontally as needed. This set-up permitted imaging of one plant every 3–4 min. Initially, 80 GS plants and 80 GR plants were planted in the field in two rows, but, owing to mortality and accidental damage during imaging process, only 63 plants of each GR and GS were imaged. Imaging took place on two consecutive days, with approximately half of the plants imaged each day between 9 a.m. and 2 p.m. The first day began with imaging of GR plants and then GS plants. The second day began with imaging of GS plants and then GR plants. Small to medium-size clouds formed occasionally as the time approached noon on both days, and the

Published 2014. This article is a U.S. Government work and is in the public domain in the USA.

data collection efforts were halted while the sun was blocked by clouds. The camera was calibrated immediately before each plant was imaged by collecting a white reference at the plant canopy. As the height of the field plants varied from 75 to 120 cm, the height of the camera was adjusted to about 66 cm above the plant canopy. It should be noted that the imaging process in the field was rugged, unlike in the greenhouse, owing to plant movement by wind and camera vibration from the engine of the tractor.

2.4 Image processing

The Pika II software (SpectrononPro v2.29-R6409; Resonon, Bozeman, MT) used in this study automatically combined white reference and dark current measurements with the images on a pixel-by-pixel basis to compute reflectance images. All reflectance images were processed to segment the plants from the background of the hyperspectral images by thresholding the band centered at 770 nm at 60% of the maximum value in the image. Plants typically reflect more light than soil in the near-infrared portion of the spectrum. The 770 nm band was chosen after tests showed that it provided good segmentation; however, other bands may provide similar results. This segmentation algorithm was effective in processing field plant images taken even under rugged conditions. After each plant was segmented out from the image, all the pixels labeled as part of the plant were combined to obtain a mean reflectance for each plant. The reflectances were then normalized to eliminate the effect of taller plants being exposed to higher light intensity. Normalization was accomplished by dividing the spectral band values by the magnitude. The magnitude was computed using the vector magnitude formula

$$|\overline{x}| = \sqrt{x_1^2 + x_2^2 + \cdots + x_n^2} \tag{1}$$

where $|\overline{x}|$ is a vector with n elements. In order to use this function, the hyperspectral bands were treated as elements of the vector. The normalized reflectance was then a unit vector ($\overline{v}$) computed by the equation

$$\overline{v} = \frac{\overline{x}}{|\overline{x}|} \tag{2}$$

2.5 Data analysis

The analysis used forward selection to select the bands, Fisher's linear discriminant analysis (FLDA) to reduce dimensionality and maximum likelihood to classify plants (these components were identical to the ones described below). The heterogeneous plants grown in the greenhouse more closely approximate the population of Palmer amaranth in agricultural fields. However, there were only 52 total plants available. The relatively small number of plants (compared with the number of spectral bands) available for this analysis limited the number of spectral bands that could be utilized before classification accuracy degraded owing to the Hughes phenomenon.[11] Hughes stated that, as the number of variables (in this case spectral bands) employed for classification increases, the number of statistical parameters (mean and covariance for each band) increases. Estimates of these parameters degrade in accuracy as the dimensionality increases, but the number of training samples does not also increase because the samples more sparsely populate the higher dimensional space. At some point the benefit obtained by adding more bands is negated by the increased error in parameter estimates. However, there were 133 plants in genetically homogeneous populations and 185 plants when both heterogeneous and homogeneous populations were combined. Pooled data permitted better estimates of statistical parameters, and thus lessened the effects of the Hughes phenomenon.

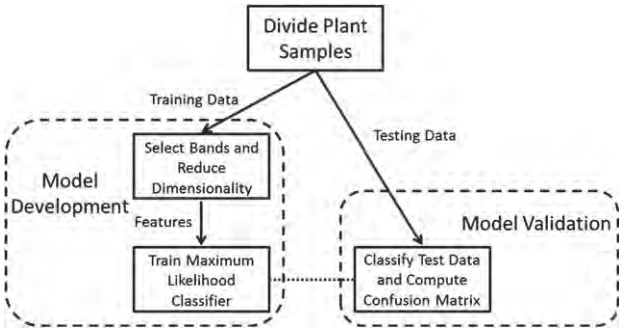

Figure 1. Flow chart of the data analysis algorithm.

The data analysis procedure is outlined in Fig. 1. Initially, the data samples were split into training and testing groups. Plants were assigned to groups randomly, with about three-quarters going to the training group (greenhouse: 66 GS, 72 GR; field: 47 GS, 47 GR), and about a quarter going to the testing group (greenhouse: 22 GS, 25 GR; field: 16 GS, 16 GR).

After the data had been assigned to groups, sensitive bands were selected using an algorithm based on the forward selection algorithm.[12] The algorithm begins with an empty set of variables (in this case, the hyperspectral bands), and iteratively adds the variable to the set that improves the preselected metric the most. In this study, the area under the receiver operating characteristic (ROC) curve was used as the metric.[13] The area under the ROC curve is a measurement of the overlap of two classes in a one-dimensional variable space. It is improved if the means of the two classes are further apart, or if the variances of one or both decreases. Both situations would provide for better classification. However, as the area under the ROC curve can only be computed for a one-dimensional variable space, a dimensionality reduction technique had to be used once the number of variables in the set grew to two or more. In this study, FLDA was used to reduce the dimensionality of the set.[14] A weighted average of the variables in the set can be expressed as

$$w_1 v_1 + w_2 v_2 + \cdots + w_n v_n = \overline{w} \cdot \overline{v} \tag{3}$$

where the weight vector $\overline{w} = \langle w_1, w_2, \ldots, w_n \rangle$ and the variable vector $\overline{v} = \langle v_1, v_2, \ldots, v_n \rangle$. Thus, the weighted average is a dot product projection of variables (the selected bands) onto the weight vector. FLDA works by choosing weights that optimize between-class scatter divided by within-class scatter. Once the weights are determined, they are used to reduce the dimensionality of the variables for each plant to a single scalar 'feature' by computing the dot product between the weight vector and variables in the set. The forward selection algorithm terminates after a predetermined number of hyperspectral bands has been selected. The number of bands varied from 1 to 20.

The next step in the model development was training the maximum likelihood (ML) classifier.[14] This involves estimating the means and variances for both GS and GR plants in the feature space, which consists of the single feature computed using the weights and selected bands obtained with FLDA. ML estimates these statistical parameters from the training data by choosing the values that have the highest probability (most log-likelihood)

Published 2014. This article is a U.S. Government work and is in the public domain in the USA.

of being the correct value. In the case of Gaussian distributions (as was assumed in this study), ML selects the sample mean and sample variance because it can be proven that these values have the greatest log-likelihood of being the actual mean and variance of the population. From the means and variances (and the Gaussian assumption), probability distributions can be estimated for GS and GR plants.

Model validation used the testing data group, which was determined when the data were split, to determine the classification accuracy. The feature developed in the model development section was computed for each testing data sample. The probability distributions estimated for GS and GR were used to estimate the probability that each testing sample was GS or GR, and they were assigned the label with the highest probability. Then, the label results were organized into confusion matrices.[12] For the combined study, a permutation study was conducted by repeating the data analysis 100 times. As the data were split randomly, different sets of plants were chosen for testing and training each time. Thereafter, the mean and standard deviation of the confusion matrices for those 100 permutations were computed.

3 RESULTS AND DISCUSSION

3.1 Hyperspectral reflectance properties of GR and GS Palmer amaranth plants

Both greenhouse- and field-grown Palmer amaranth plants have similar reflectance properties. Apparently, GS and GR plants have their own unique reflectance spectral signatures (Figs 2A and B). In general, the GS plants reflected a slightly greater portion of light in the visible part of the spectrum, while GR plants reflected a greater portion of light in the infrared part of the spectrum. There were differences in reflectance pattern between GR and GS plants, in spite of the fact that these biotypes were morphologically identical. The mechanism of resistance to glyphosate in Palmer amaranth from Georgia has been identified as amplification of the *epsps* gene[15] which encodes the enzyme 5-enolpyruvylshikimate-3-phosphate synthase target site of glyphosate. This mechanism has also been reported in GR biotypes from Mississippi,[16] in addition to reduced absorption and translocation of glyphosate.[10]

It is not clear whether and how the mechanisms of resistance may alter the reflectance properties in GR plants. Genomes of GR Palmer amaranth plants are known to have 5–160-fold more copies of the *epsps* gene than the genomes of GS Palmer amaranth plants.[15] It is postulated that amplification of the *epsps* gene may increase the carbon flow through the shikimate pathway, which may lead to an increase in downstream phenolic compounds such as coumarins, flavonoids and lignins in GR Palmer amaranth.[17] These compounds are photodynamic, and change in their endogenous levels would alter light reflectance patterns. Whether this difference in reflectance patterns between the GR and the GS plants is due to differences in their cuticular chemical composition needs further investigation. It will be interesting to investigate whether similar differences in reflectance properties are also detectable in one or more of the 24 other weed species that have evolved resistance to glyphosate.

3.2 Classification of GR and GS Palmer amaranth plants

Leave-one-out validation analyses of hyperspectral reflectance data differentiated GR Palmer amaranth from GS Palmer amaranth. The classification accuracy in the heterogeneous populations was 94.2% with 52 plants, and in homogeneous populations it was

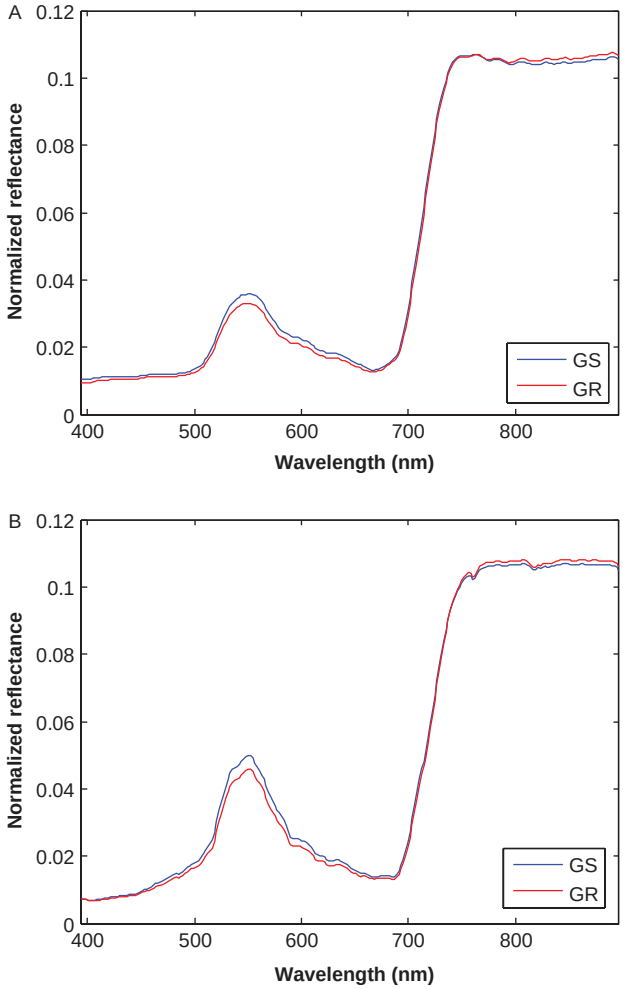

Figure 2. Plots of mean normalized reflectance signatures for the GS and GR Palmer amaranth plants: (A) mean of 88 GS and 97 GR plants grown in a greenhouse; (B) mean of 63 GS and 63 GR plants grown in the field.

100.0% with 133 plants. In the pooled populations, the classification accuracy was 93.5% with 185 plants (Table 1). The lower classification accuracy in the heterogeneous plants, raised from seed, could be due to a combination of subtle anatomical differences, existing resistance mechanism(s), segregation and other unknown factors. The homogeneous plants were all raised asexually from individual clones, thereby not 'contaminating' the original genetic make-up. The confusion matrix with prediction accuracy (as computed using leave-one-out validation) indicates how the plants of each type of Palmer amaranth were classified (Table 1). The 'GS' row of the confusion matrix describes how the GS plants were classified, and the 'GR' row describes how the GR plants were classified. The numbers in the 'GS' column indicate how many plants of each type were classified as GS, and the numbers in the 'GR' column indicate how many plants of each type were classified as GR. For example, out of the total of 27 GS plants in the heterogeneous population, 26 were (correctly) classified as GS, and one was (incorrectly) classified as GR. Typically, the 'actual' column is left out of confusion matrices because it can be computed by summing the 'GS' and 'GR' rows, while the 'prediction accuracy' is generally regarded as part of the confusion matrix. In the combined analysis, optimum classification was obtained with 14 bands (Fig. 3). The standard deviation of overall accuracy also decreases

Published 2014. This article is a U.S. Government work and is in the public domain in the USA.

Table 1. Confusion matrices and prediction accuracies in heterogeneous, homogeneous and combined populations grown in a greenhouse. These results were obtained using 14 hyperspectral bands with leave-one-out validation

	Heterogeneous				Homogeneous				Pooled			
		Predicted				Predicted				Predicted		
Palmer amaranth[a]	Actual	GS	GR	Prediction accuracy (%)	Actual	GS	GR	Prediction accuracy (%)	Actual	GS	GR	Prediction accuracy (%)
GS	27	26	1	96.3	61	61	0	100.0	88	82	6	93.2
GR	25	2	23	92.0	72	0	72	100.0	97	6	91	93.8
Overall accuracy (%)				94.2				100.0				93.5

[a] GS, glyphosate-sensitive Palmer amaranth; GR, glyphosate-resistant Palmer amaranth.

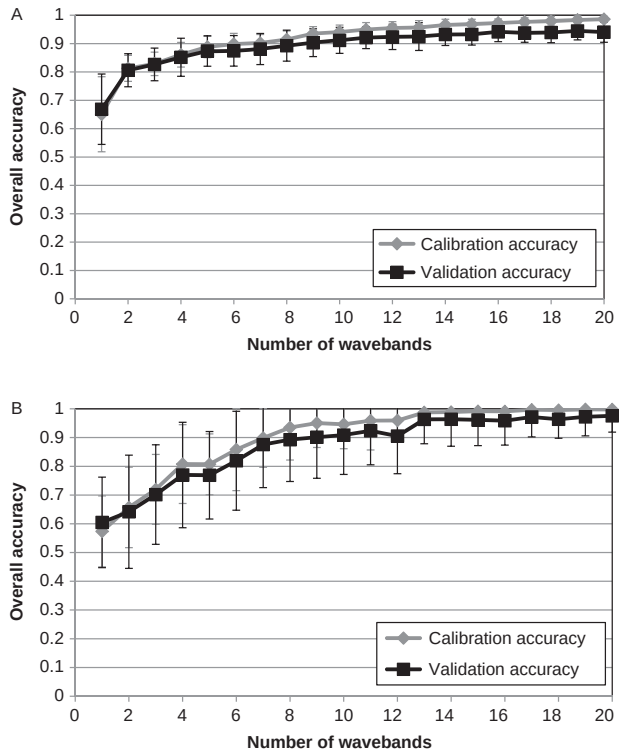

Figure 3. Plot of overall accuracy versus number of wavebands for the greenhouse plant (A) and field plant (B) analysis. The error bars indicate standard deviation.

Table 2. Confusion matrix from combined analysis of genetically heterogeneous and homogeneous plants grown in a greenhouse. Fourteen spectral bands were used in the classification of 47 unknown plants

		Predicted		
Palmer amaranth[a]	Actual	GS	GR	Prediction accuracy (%)
GS	22	20.6 (1.13)[b]	1.4 (1.13)	93.6 (5.14)
GR	25	1.5 (1.23)	23.5 (1.23)	94.0 (4.91)
Overall accuracy (%)				93.8 (3.72)

[a] GS, glyphosate-sensitive Palmer amaranth; GR, glyphosate-resistant Palmer amaranth.
[b] Values in parentheses denote the standard deviation.

Table 3. Confusion matrices and prediction accuracies in Palmer amaranth plants grown in the field. These results were obtained using 14 hyperspectral bands with leave-one-out validation

		Predicted		
Palmer amaranth[a]	Actual	GS	GR	Prediction accuracy (%)
GS	63	61	2	96.8
GR	63	2	61	96.8
Overall accuracy (%)				96.8

[a] GS, glyphosate-sensitive Palmer amaranth; GR, glyphosate-resistant Palmer amaranth.

as more bands are used. The permutation mean and standard deviation of the confusion matrix obtained with 14 bands using the pooled greenhouse data yielded a mean accuracy of about 93.8% (Table 2).

Similarly to greenhouse populations, the overall classification accuracy was 96.8% with 126 plants grown under field conditions (Table 3) using leave-one-out validation. The permutation mean and standard deviation of the confusion matrix obtained with 14 bands using the field data yielded an overall mean accuracy of about 96.4% (Table 4) and are comparable with the results in Table 2.

As the forward selection algorithm was executed on each permutation with a different set of training data, the bands used were not always the same for each permutation. Thus, the results in Tables 2 and 4 are indicative of the accuracy obtained when using the forward selection algorithm, but not of the accuracy obtained from any particular set or sets of features. When using the data from all plants to choose 14 bands, the bands indicated in Table 5 are selected for each dataset. Most of the selected bands are contained within three major clusters (Fig. 4). These clusters are 394–487 nm, 668–762 nm and 821–863 nm.

As the GS and the GR plants have different reflectance signatures (Figs 2A and B), a naive approach to distinguishing GR plants from GS plants would be to use this characteristic. However, that would neglect the role that within-class variance plays in degrading separability of GS and GR. In order to show class separation more clearly, graphs can be constructed by subtracting the combined mean normalized reflectance from the mean normalized reflectance of each class (GS and GR). As about 68% of the spectral signatures for each class will fall within these envelopes, the overlap between the two classes becomes more visible (Fig. 5). It also becomes apparent that there are four windows where there is less overlap between the classes. These windows are approximately 400–500 nm, 650–690 nm, 730–740 nm and 800–900 nm. The 14

Published 2014. This article is a U.S. Government work and is in the public domain in the USA.

Table 4. Confusion matrix from plants grown in the field. Fourteen spectral bands were used in the classification of 32 unknown plants

Palmer amaranth[a]	Actual	Predicted GS	Predicted GR	Prediction accuracy (%)
GS	16	15.5 (0.75)[b]	0.5 (0.75)	96.7 (5.39)
GR	16	0.6 (0.89)	15.4 (0.89)	96.1 (5.92)
Overall accuracy (%)				96.4 (4.69)

[a] GS, glyphosate-sensitive Palmer amaranth; GR, glyphosate-resistant Palmer amaranth.
[b] Values in parentheses denote the standard deviation.

Table 5. Central wavelengths of hyperspectral bands when all available data from greenhouse- and field-grown plants were used to select 14 bands

Dataset	Central wavelength (nm)
Heterogeneous	409 413 417 441 445 447 470 481 485 487 668 685 743 750
Homogeneous	394 396 411 554 556 712 733 739 743 825 846 853 870 897
Pooled	396 403 443 445 447 598 676 685 689 741 756 760 762 851
Field	394 399 430 445 466 682 701 714 731 821 825 830 855 863

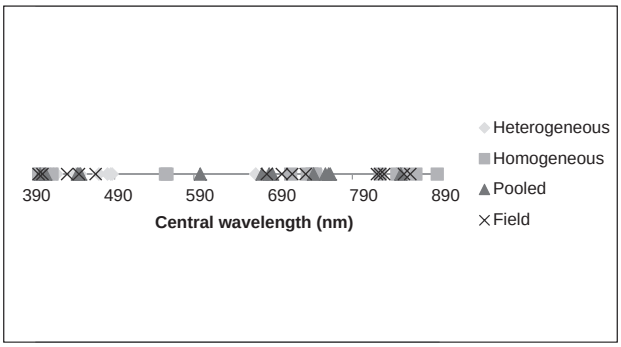

Figure 4. Number line plot of the central wavelengths of spectral bands when 14 were chosen using all the data for each plant set.

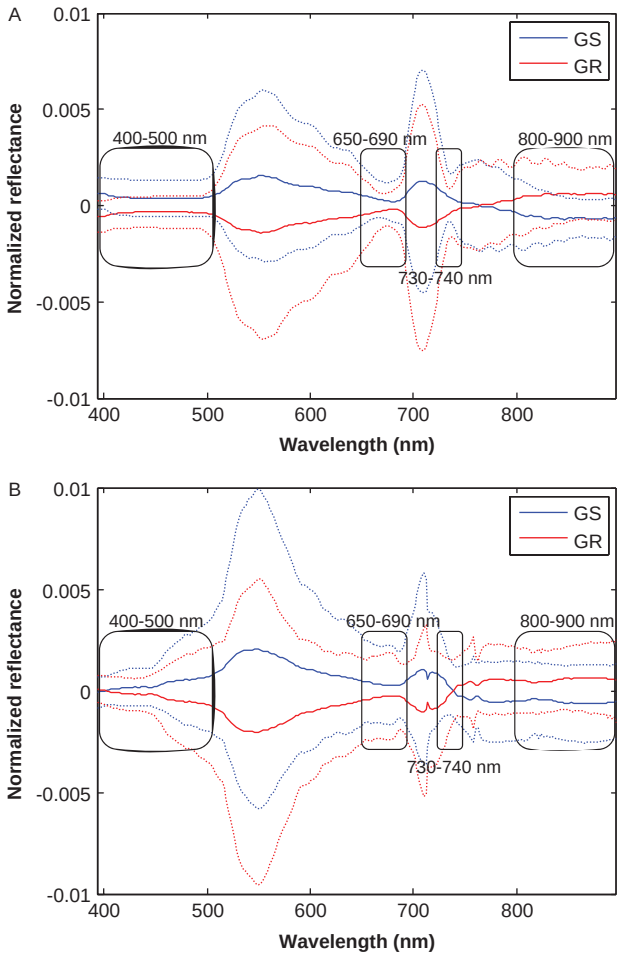

Figure 5. Illustration of separability of GS and GR plants with respect to wavelength. Solid lines indicate the mean of each class relative to the mean of all plants. The envelope shown by dotted lines indicates one standard deviation. Plot A was obtained from the greenhouse plants, and plot B from the field plants. The boxes indicate windows where the separability is best. The window between 730 and 740 nm is not as well defined in the field plants.

bands in Table 5 and Fig. 4 correlate with the clusters discovered in Fig. 5. Thus, the bands are suitable choices for this application.

The spectral reflectance signatures analyzed in this study were means of the hyperspectral pixels from the entire plant. As averaging of pixels tends to remove spatially uncorrelated noise,[18] the averaging pixel feature was computed using 14 bands for each pixel. Examples of GS and GR plant images created with feature values computed from 14 bands indicate that the difference is likely impossible to distinguish visually with the human eye in this feature space (Fig. 6). The difficulty is due to the large range of values the plant pixels can take. As histograms of the plant pixels show (Fig. 7), the feature value takes a Gaussian distribution, with most feature values ranging from about 300 to 1200 (the feature is unitless). The actual value of the feature used for classification is the mean of all the pixels in the histograms. As mean values have a smaller standard deviation,[12] the range of values for the feature used for classification is much less than the values for individual pixels. The histogram of the feature values derived from the 14 bands for all 185 plants used in the study reveals that the mean of the GR plants is about 706, and the mean of the GS plants is about 712 (Fig. 8). This means that the difference between a GS and a GR plant is about 6 units in the feature space. Because the difference is so small compared with the range of values pixels can take, it requires very precise measurements to differentiate GS from GR using a hyperspectral sensor. The segmentation algorithm also must be accurate, otherwise soil and other background pixels may influence the feature. This would possibly result in misclassifications.

The predictive model developed from greenhouse data was used to classify field-grown GR and GS Palmer amaranth plants. The classification accuracy was 55.6% (data not shown). This low classification accuracy was not surprising, as it is apparent from Figs 2A and B that there were possible calibration differences between the greenhouse and field measurements. Also, the cuticle of greenhouse- and field-grown plants would be very different, which would have a great impact on light reflectance. Although the same camera was used in both the greenhouse and the field, it should be noted that in the field the light source was natural sunlight, which interacts with the Earth's dynamic atmosphere. Furthermore, the growing conditions of the greenhouse and field plants were different. Hence, a separate model was developed

Published 2014. This article is a U.S. Government work and is in the public domain in the USA.

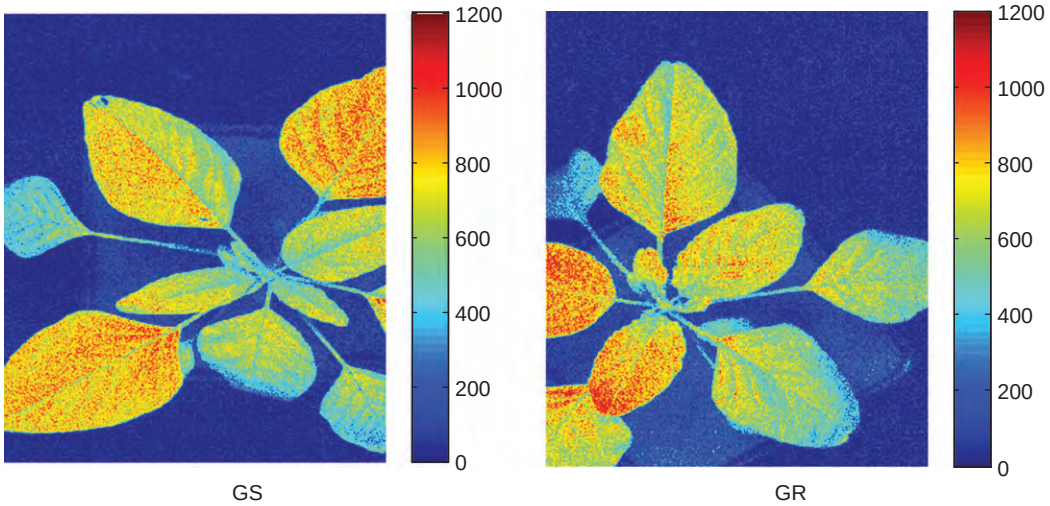

Figure 6. Images of GS and GR plants created with feature values computed from 14 bands (396, 403, 443, 445, 447, 598, 676, 685, 689, 741, 756, 760, 762 and 851 nm).

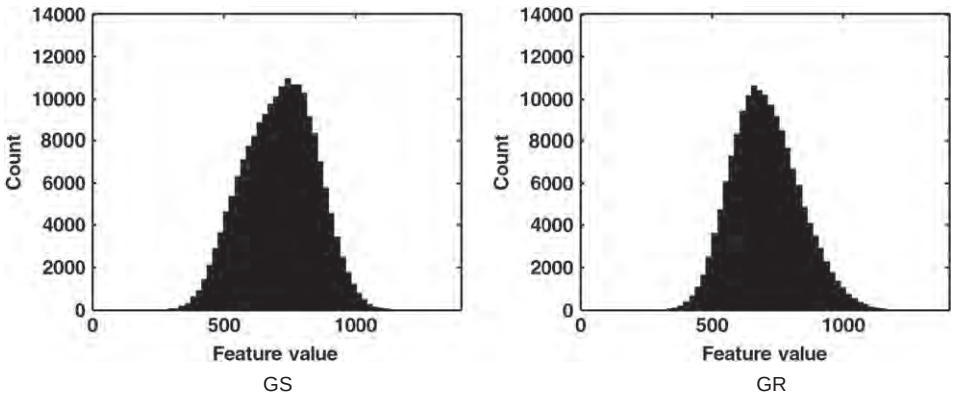

Figure 7. Histograms of the feature values computed for each pixel from a GS and GR Palmer amaranth.

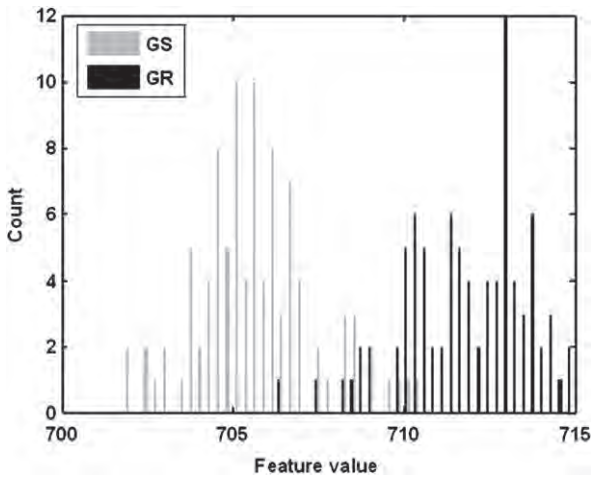

Figure 8. Histogram of mean feature values for all 185 plants grown in a greenhouse.

for field data. The classification accuracy of the field model was 96.4% (Table 4) and was comparable with the 93.8% classification accuracy of the greenhouse model (Table 2). It was conjunctured that this small difference in the predictive accuracies between greenhouse and field models is more likely due to differences in plant populations and less likely due to plant imaging conditions. Greenhouse plants included both genetically homogeneous and heterogeneous populations, whereas field plants included only a heterogeneous population.

4 CONCLUSIONS

GR and GS Palmer amaranth plants exhibit differences in hyperspectral reflectance properties. It is possible to differentiate GR and GS Palmer amaranth plants without subjecting plants to a glyphosate treatment. In general, GS plants reflect a slightly higher percentage of the total light in the visible region, and GR plants reflect a slightly higher percentage of the total light in the infrared region of the spectrum. There are four regions of the spectrum (400–500 nm, 650–690 nm, 730–740 nm and 800–900 nm) that present the best separability. There are three major clusters of selected bands when 14 are chosen for each dataset. These clusters are in the 394–487 nm, 668–762 nm and 821–863 nm regions, which correlate well with the windows of best separability. It is very likely that there exists some physiological difference between GS and GR Palmer amaranth that causes the reflectance to differ more in these areas of the spectrum. It is speculated that amplification of the *epsps* gene would be a basis for this physiological difference. This study yielded an accuracy of 93.5% or better each

Published 2014. This article is a U.S. Government work and is in the public domain in the USA.

time 14 spectral bands were chosen to predict GS and GR plants. The distributions of GS and GR in the feature space are accurately described by Gaussian distributions, which make statistical classifiers well suited for the Palmer amaranth glyphosate resistance detection problem. Hyperspectral reflectance properties of other GR and GS weed species need to be investigated to gain a better understanding of reflectance patterns between GR and GS plants and to develop a technique towards accurate classification. This hyperspectral imagery technique to identify GR and GS plants is non-destructive, does not require glyphosate treatment and has potential in practical weed management strategies.

ACKNOWLEDGEMENTS

The authors thank Efren Ford and Earl Gordon for technical assistance. Thanks also to Dr Robert Hoagland and Dr Neal Teaster for allowing leaf reflectance to be measured on GR and GS Palmer amaranth plants raised by cloning. Mention of trade names or commercial products in this publication is solely for the purpose of providing specific information and does not imply recommendation or endorsement by the US Department of Agriculture.

REFERENCES

1 Duke SO, Lydon J, Koskinen WC, Moorman TB, Chaney RL and Hammerschmidt R, Glyphosate effects on plant mineral nutrition, crop rhizosphere microbiota, and plant disease in glyphosate-resistant crops. *J Agric Food Chem* **60**:10 375–10 397 (2012).
2 Heap IM, *International Survey of Herbicide Resistant Weeds*. [Online]. Available: www.weedscience.org [16 December 2013].
3 Culpepper AS, Grey TL, Vencill WK, Kichler KM, Webster TM, Brown SM *et al*., Glyphosate-resistant Palmer amaranth (*Amaranthus palmeri*) confirmed in Georgia. *Weed Sci* **54**:620–626 (2006).
4 Norsworthy JK, Scott RC, Smith KL and Oliver LR, Response of northeastern Arkansas Palmer amaranth (*Amaranthus palmeri*) accessions to glyphosate. *Weed Technol* **22**:408–413 (2008).
5 Koger CH and Reddy KN, Role of absorption and translocation in the mechanism of glyphosate resistance in horseweed (*Conyza canadensis*). *Weed Sci* **53**:84–89 (2005).
6 Shaner DL, Nadler-Hassar T, Henry WB and Koger CH, A rapid *in vivo* shikimate accumulation assay with excised leaf discs. *Weed Sci* **53**:769–774 (2005).
7 Mahlein A-K, Steiner U, Hillnhutter C, Dehne H-W and Oerke E-C, Hyperspectral imaging for small-scale analysis of symptoms caused by different sugar beet diseases. *Plant Meth* **8**:3 (2012).
8 Huang Y, Bruce LM, Koger T and Shaw D, Analysis of the effects of cover crop residue on hyperspectral reflectance discrimination of soybean and weeds via Haar transform. *2001 IEEE Int Geosci Remote Sensing Symp* **3**:1276–1278 (2001).
9 Thorp KR and Tian LF, A review on remote sensing of weeds in agriculture. *Precision Agric* **5**:477–508 (2004).
10 Nandula VK, Reddy KN, Koger CH, Poston DH, Rimando AM, Duke SO *et al.*, Multiple resistance to glyphosate and pyrithiobac in Palmer amaranth (*Amaranthus palmeri*) from Mississippi and response to flumiclorac. *Weed Sci* **60**:179–188 (2012).
11 Hughes G, On the mean accuracy of statistical pattern recognizers. *IEEE Trans Inf Theory* **14**:55–63 (1968).
12 Montgomery DC and Runger GC, *Applied Statistics and Probability for Engineers*, 3rd edition. John Wiley & Sons, Inc., New York, NY (2003).
13 Green DM and Swets JA, *Signal Detection Theory and Psychophysics*. John Wiley & Sons, Inc., New York, NY (1966).
14 Duda RO, Hart PE and Stork DG, *Pattern Classification*. 2nd edition. John Wiley & Sons, Inc., New York, NY (2001).
15 Gaines TA, Zhang W, Wang W, Bukun B, Chisholm ST, Shaner DL *et al.*, Gene amplification confers glyphosate resistance in *Amaranthus palmeri*. *Proc Natl Acad Sci USA* **107**:1029–1034 (2010).
16 Ribeiro DN, Pan Z, Duke SO, *Nandula VK*, Baldwin BS, Shaw DR *et al.*, Involvement of facultative apomixis in inheritance of *EPSPS* gene amplification in glyphosate-resistant *Amaranthus palmeri*. *Planta* **239**:199–212 (2014).
17 Dewick PM, The shikimate pathway: aromatic amino acids and phenylpropanoids, in *Medicinal Natural Products*, 2nd edition. John Wiley & Sons, Ltd, Chichester, UK, pp. 121–166 (2002).
18 Gonzalez RC and Woods RE, *Digital Image Processing*, 2nd edition. Prentice-Hall, Inc., Upper Saddle River, NJ (2002).

 Published 2014. This article is a U.S. Government work and is in the public domain in the USA.